

## Review Article

## Open Access

## Standard Method for the Determination of the Photocatalytic Activity of Titanium Dioxide $\text{TiO}_2$ in a Black Body Reactor

S Ahmed\*, L A Al-Hajji, Adel Ismail, M Alsaidi and A Alduweesh

Nanotechnology and Advanced Materials Program, Research Center of Energy and Building, Kuwait Institute for Scientific Research, Safat 13109, Kuwait

### ABSTRACT

Synthesis of semiconductors to be used as photocatalysis, solar fuels attracts a wide attention since semiconductors photocatalyst are the most effective techniques to harvest solar light for environmental remediation. To determine the activity of a semiconducting photocatalyst is by employing a black body photoreactor, where is the reaction rate defined as the converted amount of a probe molecule per unit time ( $dn/dt$ ). measuring the reaction rate of a probe compound with the same type of photoreactor to compare the activities of photocatalysts under identical irradiation conditions is a very general way. The black body like a reactor is a new practical application to measure the quantum yields of photochemical reactions ( $\Phi$ ) in liquid-solid heterogeneous systems. One of the most major advantage of this new method, it is too simple to determine the photocatalytic activity of a photocatalysts such as the  $\text{TiO}_2$  as long as the fraction of the reflected and transmitted light are negligible due to the reactor geometry and high optical density of the heterogeneous systems. The quantum yields of the heterogeneous system is a direct reaction since there is a lack of reliable experimental methods which make the determination at any photocatalytic laboratories very easy. The quantum yields are defined as the number of molecules of a given reactant per photon of light absorbed by photocatalyst at a given wavelength.

### \*Corresponding author

S Ahmed, Nanotechnology and Advanced Materials Program, Research Center of Energy and Building, Kuwait Institute for Scientific Research, Safat 13109, Kuwait. E-mail: shmed@kisr.edu.kw

Received: June 14, 2022; Accepted: June 21, 2022; Published: July 26, 2022

**Keywords:** Semiconductors, Photocatalyst, Black Body Photoreactor, Quantum Yields, Heterogeneous, Reaction Rate

### Introduction

In the early 1970s, Solonitsyn and Basov<sup>5</sup> were the first to introduce the application of black body reactor for measuring the quantum yield of a photoreaction but in gas-solid heterogeneous systems for example, photostimulated absorption of oxygen, hydrogen and methane on  $\text{ZnO}$  and  $\text{TiO}_2$  also for other metal oxides. The light beam is directed through the small area of inlet window (diameter 2mm), into the inner sphere (diameter 25mm). the space (thickness of 3-5 mm), between the inner and the outer walls of the reactor is filled with the catalyst powder. In the application of the black body reactor the fraction of the transmitted light is zero due to the high optical density, that's ( $T \rightarrow 0$ ). Since the area of the inlet window is too small comparing to the total area of the inner cavity of the reactor, loss of light due to back reflection through the inlet window is assumed as zero, that's ( $R \rightarrow 0$ ). The light inside the reactor, it undergoes multiple stages of scattering and reflections, before it is finally absorbed by the photocatalyst, therefore we can assume that all the emitted light into the inner cavity of the reactor is totally absorbed by the photocatalyst ( $A \rightarrow 1$ ). In other words experimental determination of the quantum yield is the reaction rate and the light intensity at the inlet window of the reactor. Practically, one more issue has to be done correctly for the determination of the quantum yield, is to assure that the surface of the photocatalyst is uniformly irradiated. In the case of the black body reactor and for the majority of the other reactors, this condition is hard to fulfil because the

surfaces of the different particles of the photocatalyst are exposed to different intensities of the incident light. Basov and his co-worker approved that the determination of the quantum yield in a non-uniformly irradiated heterogeneous system is practically corresponded to the true quantum yield as the reaction rate scales linearly with light intensity.

The main advantage of this application is its simplicity since the fractions of the reflected and transmitted light is considered as zero, Due to the reactor geometry, and the high optical density of the heterogeneous system. This means that all the photons at suitable wavelengths emitted by the light source and directed to the suspension are absorbed by the photocatalyst. The reaction rates define as the amount of the probe molecule per time.

The major obstacle in determining the quantum yields of heterogeneous photoreaction is how to estimate the exact number of photons that been actually absorbed by the solid photocatalyst. Fractions of reflected ( $R$ ), transmitted ( $T$ ), and absorbed ( $A$ ) light in the heterogeneous photoreaction system follow the conservation law. To determine the fraction of the absorbed light it is necessitate knowledge to know the fraction of the reflected and transmitted light. The diffuse scattering of light in dispersed photocatalytic systems, problem limits the determination of these fractions, which in turn required more sophisticated means. To come over this problem many researcher and workers report the quantum yield on the basis of incident light rather than the actual absorbed light by the heterogeneous system.

In the heterogeneous system. The best method to know the perfect photocatalyst, is to compare the activities of two or more of photocatalysts by measuring the reaction rates of one chosen probe compound under the same type of photoreactor and applying exactly the same experimental conditions. Comparability should be fulfilled with at least five conditions. For examples:

- Reaction rates should not be affected by the numbers of PHOTONS been SCATTERED out of the photoreactor.
- The reaction rates should be independent of the photoreactor geometry.
- The reaction rates should be independent of the suspension volume.
- The concentration of the probe compound.
- The reaction rates should be independent of the mass concentration of the chosen photocatalyst.

All the conditions are fulfilled within the limit of experimental error. in characterizing the activity of a certain photocatalyst, the reaction rate and the quantum yield are independent of the reagent concentration so that the efficiency of the heterogeneous system depends only on activity of the photocatalyst. As previously mentioned, the reaction rate is independent from the concentration of the probe compound (dichloroacetic acid or the phenol). Since this last one concentration is sufficiently large ( $K_c \gg 1$ ), the fractions of reflected and transmitted light in a black body reactor are zero, the kinetics of this reaction rates is zero, ( $\frac{dn}{dt} = V_{dc}/V_{dt} = V_k$ ). At high photocatalyst concentration ,the total number of photons absorbed by the photocatalyst per unit time remains constant [1-5].

## Experimental

In this study the initial concentration of the probe compound  $C_0$ , the mass concentration of the heterogeneous photocatalyst, and the suspension volume (v) on the rate of the photocatalytic degradation of dichloroacetic acid (DCA) has been investigated.

The degradation of the dichloroacetic acid over  $\text{TiO}_2$  nanoparticles was chosen as the test reaction. All reagents were from (Aldrich; purity>99%), Merck, Fluka, Roth) The suspension was prepared by dissolving 10 mM of dichloroacetic acid and  $\text{KNO}_3$ , resulting in solution with 10mM of Potassium nitrate and varying concentration of the probe compound (2mM-to 20mM).  $\text{TiO}_2$  nanoparticles was used as the photocatalyst. The role of using the potassium nitrate is to keep the ionic strength constant. The resulting suspension was stirred in dark for 2hr with the PH 3 by addition of KOH, in order to establish the adsorption equilibrium. The reaction was performed in a glass bottle, filled with the resulting suspension which was irradiated with monochromatic light source (Omicron laserage laserprodukte GmbH,  $\lambda_{max} = 365\text{nm}$ ) with full width at half maximum=10nm as determined ith B&W Tek Spectra Red xpress ,photon flux=12 $\mu\text{mol min}^{-1}$  as determined by ferrioxalate actinometry). LED lamp connected to a suitable wave guide within a glass tube (outer diameter=11mm,inner diameter 9 mm) the exit of the wave guide was placed in the center of the reactor. The light source was switched on and the suspension was irradiated for 3hr and samples were taken at 30 minute intervals, then centrifuged for 5 minutes at 13000 rpm. The supernatant solutions were filtered through syringe filters with 0.2  $\mu\text{m}$  pore size and diluted 20 times.

Quantitative analysis of dichloroacetic acid was performed by high performance ion chromatography (HPIC) employing a dionex

ICS-1000 instrument equipped with an anion exchange column (Ion Pac AS9-HC 2X250mm) in combination with a guard column (Ion Pac AG9-HC 2X50mm).the aqueous mobile phase contained 8 mM  $\text{NaCO}_3$  and 1.5 mM  $\text{NaHCO}_3$ . The flow rate of the mobile phase was set to 0.3  $\text{mL min}^{-1}$ , and the applied column temperature was 35°C.

## Results and Discussions

### Structural Characterizations

#### As-Synthesized $\text{TiO}_2$ Nanoparticles

#### Powder X-Ray Diffraction (Xrd)

The structural changes of  $\text{TiO}_2$ , composite was investigated by XRD. All the samples were analyzed with a speed of 20/min via continuous 20/θ scan mode, using CuKα radiation ( $\lambda=0.15418\text{ nm}$ ) operating at 45 kV 200 mA. A high-speed 1D X-ray detector D/teX Ultra 1D mode (D/teX) with Ni Filter was used. The diffraction patterns were obtained over the 20 range of 20° to 80° with a step size of 0.02/ 20 and a time of 1 s/step, as shown in Fig. 1. The XRD resulted from constructive and destructive interference caused by scattering of X-rays from atoms in a regular array, with diffraction lines appearing at angles that satisfy Bragg's law (Eq. 1)

$$n\lambda = 2d \sin\theta \quad (1)$$

Where n is the order of diffraction,  $\lambda$  the x ray wavelength, d the inter planar spacing, and  $\theta$  the angle of diffraction.

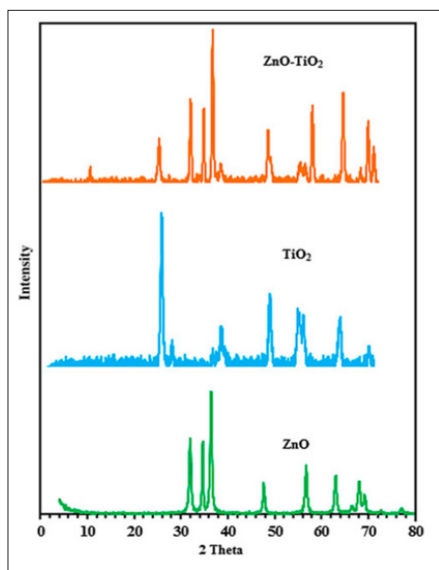
### Ft-IR Analysis

The reaction mostly occurs on the surface of the photocatalyst. FT-IR at a certain range of 400-4,000  $\text{cm}^{-1}$  as shown in figure 2 is recommended for analyzing  $\text{ZnO}/\text{TiO}_2$  composite. The  $\text{ZnO}$  perfect absorption peaks were observed at 455,725,915, and 3,477  $\text{cm}^{-1}$ . Whereas the band observed between 400-500  $\text{cm}^{-1}$  is corresponding to the stretching vibration of  $\text{ZnO}$ . The weak band related to H-O-H near 1,590  $\text{cm}^{-1}$  is bending vibration. Some moisture was adsorbed on the FT-IR sample disk when prepared in an open-air atmosphere. The band at 3,500  $\text{cm}^{-1}$  is corresponding to the hydroxyl groups (-OH). The band at 478 $\text{cm}^{-1}$  can be related to the pure  $\text{ZnO}$ .  $\text{TiO}_2$  nanoparticles, peaks related to the stretching vibration and bending vibration mode respectively, at 433, and 617  $\text{cm}^{-1}$  (Gholami, Siboni, Farzadkia, and KyuYang2015).

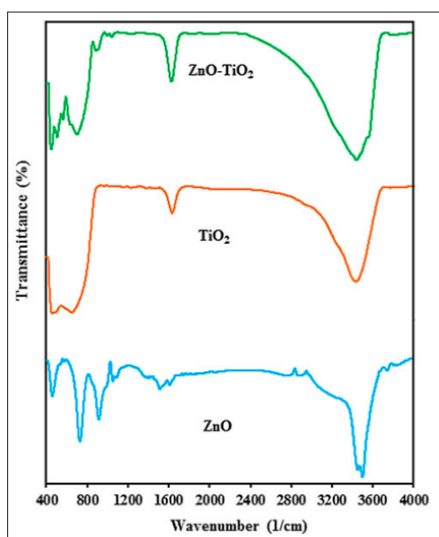
### Morphological Characterizations

Field Emission Scanning, Electron Microscopy (FESEM). FESEM/ EDS, using JEOL: JSM-7800F operated at an acceleration power of 15 kV was used to investigate the morphological characterizations of the samples and the powder elemental analysis, including powder shape and particle size. The powder samples coated with double-sided adhesive carbon tape and placed on a Cu-sample holder. The coated samples were inserted into the FESEM chamber for analysis.

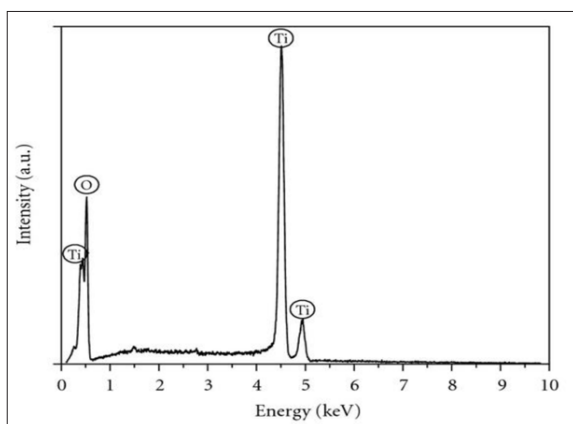
FE-SEM can obtain the surface of  $\text{ZnO}$  nanoparticles and  $\text{ZnO}/\text{TiO}_2$  nanoparticles using an EDX. SEM images of  $\text{ZnO}$  nanoparticles and  $\text{ZnO}/\text{TiO}_2$  nanoparticles are shown in Figure 3. The purpose of the EDX microanalysis to characterize the elemental composition of the nanocomposite. According to the results of the EDX analysis, the major elements were Zn (31,50%), O (14,41%), and Ti (7,30%). these results indicate good hybridization between  $\text{ZnO}$  and  $\text{TiO}_2$ , (Gholami, Siboni, Farzadkia, and KyuYang2015).



**Figure 1:** X-Ray diffraction patterns of  $\text{TiO}_2$ ,  $\text{ZnO}$  and  $\text{ZnO-TiO}_2$  as prepared nanoparticles using sol gel technique

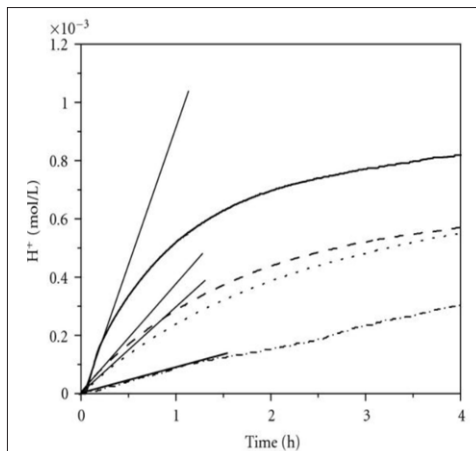


**Figure 2:** Fourier-transform infrared spectroscopy FT-IR spectra of samples SEM analysis



**Figure 3:** Energy Dispersive X-Ray Spectroscopy (EDX) spectrum of  $\text{TiO}_2$  nanoparticles used on the photodegradation of dichloroacetic acid

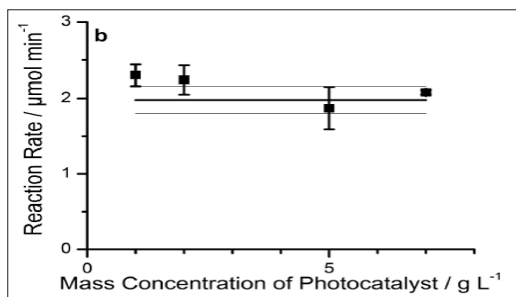
## Chromatography Results



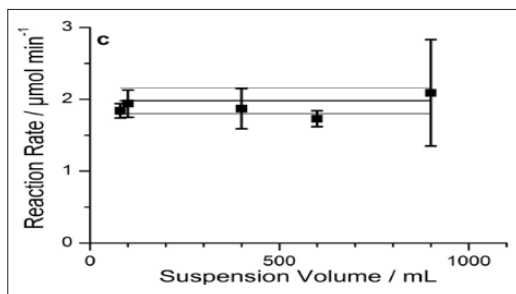
**Figure 4:** High performance ion chromatography (HPIC), the degradation of dichloroacetic acid using the photocatalyst  $\text{TiO}_2$  nanoparticles at pH 3

Figure 2: (a) Degradation of DCA (shown as release of  $\text{H}^+$ ) using the photocatalyst  $\text{TiO}_2$  nanoparticles at pH 3 in 3 consecutive runs, 1st run (—), 2nd run (---), 3rd run (···), a 3rd run (---) with addition of 4 mM  $\text{Cl}^-$  before the run started, and slope ( ) used for the determination of the photonic efficiency of each run with  $I \approx 3.39 \times 10^{-2}$  Einstein  $\text{L}^{-1}\text{h}^{-1}$ . The photocatalyst loading was 0.5 g/L. (b) Degradation of DCA (shown as release of  $\text{H}^+$ ) using the photocatalyst  $\text{TiO}_2$  nanoparticles at pH 3 in 3 consecutive runs with intermittent washing between the runs, 1st run (—), 2nd run (---), 3<sup>rd</sup> run (···), and slope ( ) used for the determination of the photonic efficiency of each run with  $I \approx 3.39 \times 10^{-2}$  Einstein  $\text{L}^{-1}\text{h}^{-1}$ . The photocatalyst loading was 0.5 g/L.

## Operational Parameters Effects



**Figure 5:** the reaction rate was independent of the concentration of the photocatalyst. It shows that the rate  $dn/dt$  is not affected by increasing the catalyst concentration. The average reaction rate is  $1.89 \pm 0.10 \mu\text{mol min}^{-1}$ .



**Figure 6:** The reaction rate was independent of the suspension volume. It shows that the rate  $dn/dt$  is not affected by changing the suspension volume  $V$ . Average reaction rates  $2.12 \pm 0.15 \mu\text{mol min}^{-1}$

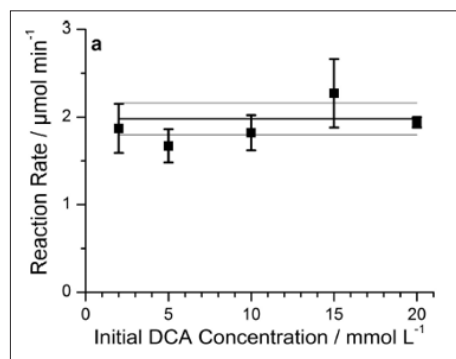


**Figure 7:** As can be seen, the reacted amount of the probe compound per unit time is constant and the reaction rate is not affected by the initial concentration  $c_0$  of the probe molecule when  $c_0 \geq 2$  mM. The average rate was calculated to be  $1.91 \pm 0.15 \mu\text{mol min}^{-1}$ .

In this study the effect of the initial concentration  $c_0$  of the probe molecule, the mass concentration  $g$  of the heterogeneous photocatalyst, and the suspension volume  $V$  on the rate of the photocatalytic degradation of dichloroacetic acid (DCA) have been investigated. The rates were measured employing black body photoreactor in which the light entrance is surrounded by a sufficient amount of suspension in all three spatial directions to guarantee the complete absorption of the slopes of the concentration vs. time plots of the experimental runs have been used to calculate the rates on an amount basis ( $dn/dt = Vdc/dt$ ). The thus calculated rates are presented in Figure 1. As can be seen Figure 7, the reacted amount of the probe compound per unit time is constant and the reaction rate is not affected by the initial concentration  $c_0$  of the probe molecule when  $c_0 \geq 2$  mM. The average rate was calculated to be  $1.91 \pm 0.15 \mu\text{mol min}^{-1}$ . Figure 5 and 6 reveal that the rates  $dn/dt$  are neither affected by increasing the catalyst concentration  $g$  nor by changing the suspension volume  $V$ . Average reaction rates of  $1.89 \pm 0.10 \mu\text{mol min}^{-1}$  and  $2.12 \pm 0.15 \mu\text{mol min}^{-1}$  were calculated. The average value for the reaction rate of all experimental runs performed with UV 100 in this study ( $N=12$ ) was calculated to be  $1.98 \pm 0.18 \mu\text{mol min}^{-1}$  [6-9].

## Conclusion

Application of the black body like reactor has been established for the first for measuring the quantum yield of photochemical reactions in liquid-solid heterogeneous systems.

Simplicity is the most advantages of the black body like reactor in a liquid-solid heterogeneous system due to the reactor geometry and that the reflection and the transmittance of light  $R$ , and  $T$  can always be taken as zero,  $R \rightarrow 0$ ,  $T \rightarrow 0$ .

The irradiated light directed inside the heterogeneous system, thus that the absorbance  $A \rightarrow 1$ .

Determination of quantum yield is simply a measurement of reaction rates and the irradiance of the actinic light which can easily established at any photochemical laboratory.

## Acknowledgements

Appreciation is extended to the Kuwait Foundation for the Advancement of Sciences (KFSAS) for the partial financial support of this study related to the Project EA071C. The financial support received by the Kuwait Government through the Kuwait Institute for Scientific Research for purchasing the equipment used in the

present work, using the budget dedicated for the project led by the first author of Establishing Nanotechnology Center in KISR is highly appreciated.

## References

1. H Kisch, D Bahnemann (2015) *J. Phys.Chem Lett.* H.kisch, semiconductor photocatalysis. Principles and applications, Wiley-VCH, Weinheim, Germany 6: 1907-1910.
2. M Sherif El-Eskandarany (2015) Mechanical Alloying, Nanotechnology, Materials Science and Powder Metallurgy, Elsevier, Oxford, UK 2nd ed.
3. W Klement, R H Willens, P Duwez (1960) Non-crystalline structure in solidified gold-silicon alloys, *Nature* 187: 869-870.
4. H Kisch (2015) semiconductor photocatalysis. Principles and applications, Wiley-VCH, Weinheim, Germany 264.
5. Árpád Molnáar, Gerard V Smith, Mihály Bartók (1989) New Catalytic Materials from Amorphous Metal Alloys, *Advances in Catalysis* 36: 329-383.
6. I P Jain, Chhagan Lal, Ankur Jain (2010) Hydrogen storage in Mg: A most promising material, *Int J Hydrogen Energy* 35: 5133-5144.
7. M Sherif El-Eskandarany, Ehab Shaban, Badryiah Al-Halaili (2014) Nanocrystalline  $\beta$ - $\gamma$ - $\beta$  cyclic phase transformation in reacted ball milled MgH<sub>2</sub> powders 39: 12727-12740.
8. H Shao, G Xin, J Zheng, X Li, E Akiba (2012) Nanotechnology in Mg-based materials for hydrogen storage, *Nano Energy* 1: 590-601.
9. C X Shang, M Bououdina, Y Song, Z X Guo (2004) Mechanical alloying and electronic simulations of (MgH<sub>2</sub>+M) systems (M = Al, Ti, Fe, Ni, Cu and Nb) for hydrogen storage, *Int J Hydrogen Energy* 29: 73-80.

**Copyright:** ©2022 S Ahmed, et al. This is an open-access article distributed under the terms of the Creative Commons Attribution License, which permits unrestricted use, distribution, and reproduction in any medium, provided the original author and source are credited.